Solid State Communications 151 (2011) 1953–1957

Contents lists available at SciVerse ScienceDirect

Solid State Communications

journal homepage: www.elsevier.com/locate/ssc

Probing into the effect of Auger recombination mechanism on zero bias resistance–area product in $In_{1-x}Ga_xAs$ detector

Yuchun Chang [a], Bao Shi [a], Longhai Li [a], Jingzhi Yin [a,*], Fubin Gao [a], Guotong Du [a], Yixin Jin [b]

[a] State Key Laboratory on Integrated Optoelectronics, College of Electronic Science and Engineering, Jilin University, 2699 Qianjin Street, Changchun, 130012, People's Republic of China

[b] Changchun Institute of Optics, Fine Mechanics and Physics, Chinese Academy of Sciences, Changchun, 130033, People's Republic of China

ARTICLE INFO

Article history:
Received 19 October 2010
Received in revised form
5 August 2011
Accepted 20 September 2011
by X.C. Shen
Available online 24 September 2011

Keywords:
A. $In_{1-x}Ga_xAs$ detector
D. Auger recombination mechanism
D. R_0A

ABSTRACT

D^* (Detectivity), an important figure of merit for photodetectors, is limited by zero bias resistance–area product (R_0A). R_0A is determined by Auger recombination mechanism, depending on the composition, temperature, carrier concentration and other parameters of the photodetectors. To investigate R_0A of $In_{1-x}Ga_xAs$ infrared photodetectors, in this paper, theoretical analysis of Auger recombination mechanism was carried out in the room temperature, by taking CCCH, CHHL and CHHS into account. The calculated results show that there are significant influences on R_0A for various parameters in both p- and n-type regions of the devices. With carrier concentration around 10^{17} to 10^{18} cm^{-3}, R_0A of 10^8 Ω cm^2 (n-region) and 10^6 Ω cm^2 (p-region) are obtained for $x = 0.47$, when thickness and surface recombination velocity of the sample are 5 μm and 100 m/s, respectively.

1. Introduction

Optical detection is indispensable for optoelectronic applications, such as image sensing, fiber communications, bio-medical applications, etc. Due to fast transient response, high-sensitivity, low dark current, as well as easy integration, InGaAs infrared photodetectors have attracted more research interests recently, especially in high-performance infrared and uncooled focal plane arrays, applied in laser radar, infrared imaging and other fields [1–4].

One important parameter for detectors is detectivity, denoted as D^*. It is the normalized signal-to-noise ratio of a detector that represents the ability of the device to detect weak optical signals. Because of statistical nature of generation–recombination (g–r) processes in photodetectors, there are various noise generation mechanisms in the devices, including generation–recombination noise, tunneling noise, radiative noise, and Auger recombination noise. However, process related mechanisms (Shockley–Read–Hall, generation at surfaces and interfaces, tunnel generation and others) can be eliminated or reduced by the progress of epitaxy and devices fabrication techniques [5]. Hence Auger recombination plays a dominant role in well-designed devices [6–8].

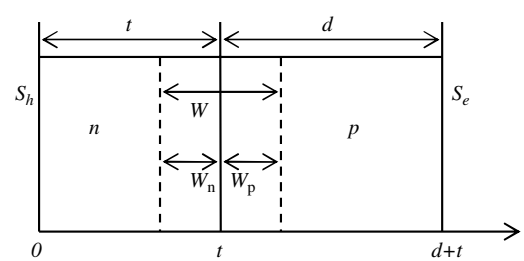

Fig. 1. Schematic of p–n junction for InGaAs detector.

In this paper, we investigated Auger recombination mechanism in $In_{1-x}Ga_xAs$ infrared photodetectors by means of theoretical analysis and comprehensive calculation of the dependence of zero bias resistance–area product (R_0A) on material parameters. Here, R_0A is proportional to the square of D^* when assuming that the quantum efficiency η is a constant.

2. Theoretical analysis

The detector studied here consisted of the homogeneous n–p type of $In_{1-x}Ga_xAs$ deposited on InP substrate. Its structure is shown in Fig. 1. S_e and S_h are the surface recombination velocity of the electron and hole, respectively.

The basic expression of the detector D^* under negligible background radiation and at zero bias voltage is given by Tian

* Corresponding author. Tel.: +86 431 85168359; fax: +86 431 85168270.
E-mail address: yjz886666@yahoo.com.cn (J. Yin).

0038-1098/$ – see front matter © 2011 Elsevier Ltd. All rights reserved.
doi:10.1016/j.ssc.2011.09.014

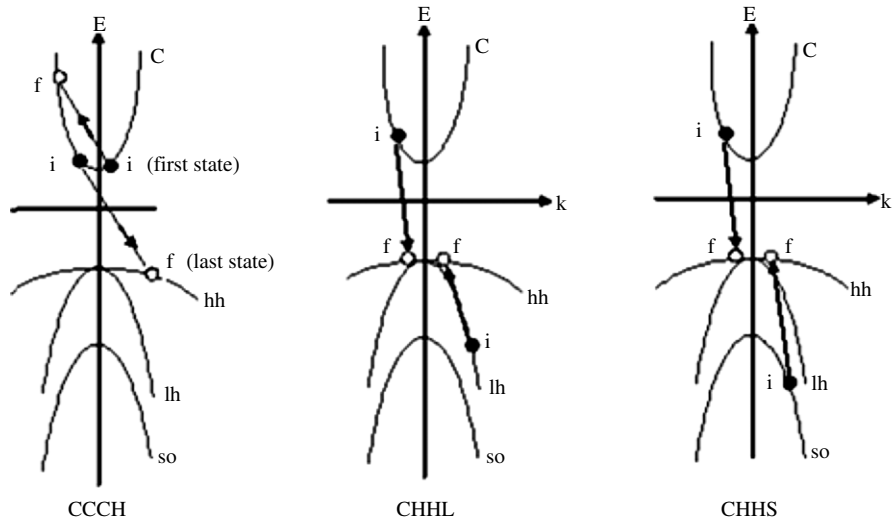

Fig. 2. The recombination process of CCCH, CHHL, CHHS.

et al. [9]:

$$D^* = \frac{\lambda \eta q}{hc}\sqrt{\frac{R_0 A}{4kT}} \tag{1}$$

where R_0A is the product of resistance at zero bias voltage and detector area, k is the Boltzmann constant, T is the temperature, λ is the wavelength of the incidence light, η is the quantum efficiency, q is the charge of an electron and c is the velocity of light.

According to the theory of the semiconductor, photo-absorption occurs only when incident light wavelength λ is shorter than the cutoff wavelength λ_c. Assuming that the maximum wavelength of the incidence light $\lambda = \lambda_c = hc/E_g$ (E_g is the bandgap of the material) and quantum efficiency $\eta = 1$, Eq. (1) can be simplified as follows:

$$D^* = \frac{q}{E_g}\sqrt{\frac{R_0 A}{4kT}}. \tag{2}$$

Obviously, E_g is a constant when temperature and material composition are fixed. Thus, D^* is determined only by R_0A which is related to various kinds of noise mechanisms. We assume only diffusion current caused by the minority carrier and the device is an abrupt junction under low-injection condition. R_0A can be expressed in Auger recombination mechanism as follows in the p- and n-regions, respectively [9].

$$(R_0A)_e = \frac{kT}{q^2}\frac{L_e p}{D_e n_i^2} \times \frac{r_e sh\left(\frac{d-w_p}{L_e}\right) + ch\left(\frac{d-w_p}{L_e}\right)}{r_e ch\left(\frac{d-w_p}{L_e}\right) + sh\left(\frac{d-w_p}{L_e}\right)} \quad \text{(p-region)} \tag{3}$$

$$(R_0A)_h = \frac{kT}{q^2}\frac{L_h n}{D_h n_i^2} \times \frac{r_h sh\left(\frac{t-w_n}{L_h}\right) + ch\left(\frac{t-w_n}{L_h}\right)}{r_h ch\left(\frac{t-w_n}{L_h}\right) + sh\left(\frac{t-w_n}{L_h}\right)} \quad \text{(n-region)} \tag{4}$$

where $D_i = \frac{kT}{q}\mu_i$, $L_i = (D_i\tau_i)^{1/2}$, $r_i = \frac{L_i S_i}{D_i}$, ($i = e$ or h). D_i, L_i, and μ_i are the diffusion coefficient, diffusion length, and effective mobility, respectively; τ_i is the lifetime of the minority carrier, n and p are the majority carrier concentration in the n-type and p-type regions, respectively. Both Eqs. (3) and (4) show R_0A are influenced by material parameters, especially by the minority carrier lifetime, through the minority recombination process.

As discussed previously, for a well-designed device, only Auger recombination mechanism is considered. Auger recombination is the non-radiating transition process among the heavy, light hole and conduction bands in semiconductors, with three particles involved in ten ways [10]. Basically, CCCH and CHHL are two fundamental Auger recombination mechanisms. However, in the narrow bandgap semiconductors, the spin–orbit split-off (Δ) is close to the bandgap of the material, therefore, the spin–orbit split-off band is more important than the light hole one, leading to CHHS should be considered [11,12]. Fig. 2 shows CCCH, CHHL, CHHS recombination processes.

The lifetimes of CCCH, CHHL, and CHHS are indicated by Tian et al. [9]

$$\tau_{CCCH} = \frac{2\tau^i_{CCCH}}{1 + n_0/p_0} \tag{5}$$

$$\tau_{CHHL} = \frac{2\tau^i_{CHHL}}{1 + p_0/n_0} \tag{6}$$

$$\tau_{CHHS} = \frac{2\tau^i_{CHHS}}{1 + p_0/n_0}. \tag{7}$$

The total Auger lifetimes τ_A is

$$\frac{1}{\tau_A} = \frac{1}{\tau_{CCCH}} + \frac{1}{\tau_{CHHL}} + \frac{1}{\tau_{CHHS}} \tag{8}$$

where p_0 and n_0 are the hole and the electron carrier concentrations at equilibrium state in the same material, respectively, and τ^i indicates the intrinsic recombination time [13,14].

The ternary-alloy material parameters used in simulation are obtained by linear interpolation of GaAs, InAs alloys parameters, given in Table 1.

3. Calculation results and discussions

The dependence of τ_{CCCH}, τ_{CHHL}, τ_{CHHS} on Ga composition with the certain carrier concentration at 300 K in $In_{1-x}Ga_xAs$ detector is calculated. It is shown in Figs. 3 and 4.

From the figures, it can be seen that Auger recombination lifetime in both p- and n-type regions increases with Ga composition. This is because the bandgap changes with Ga composition. As the bandgap becoming wider, the probability

Table 1
List of the material parameters used of binary alloys.

Alloy	$E_g(T)$ (eV)	Δ	m_e^*/m_0	m_h^*/m_0	m_s^*/m_0	ε_r
GaAs	$1.519 - 5.4010^{-4}T^2/(T+204)$	0.34	0.067	0.45	0.15	13.18
InAs	$0.420 - 2.5010^{-4}T^2/(T+75)$	0.38	0.023	0.41	0.089	14.5

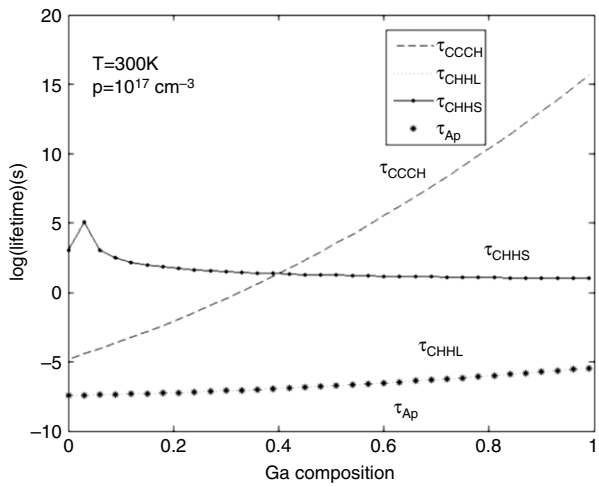

Fig. 3. The dependence of Auger recombination lifetime on Ga composition in p-region at $T = 300$ K, $p = 10^{17}$ cm^{-3}.

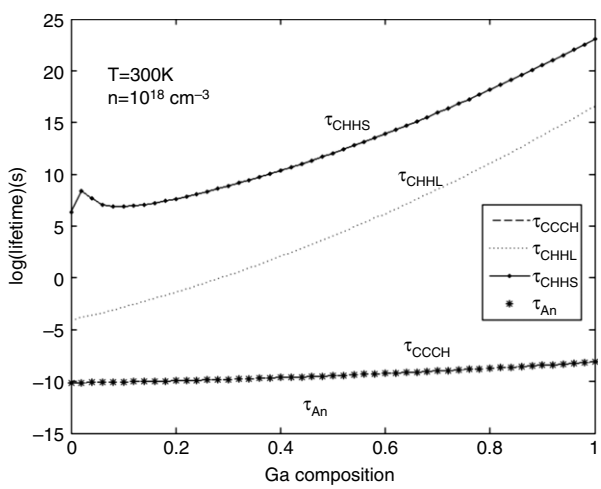

Fig. 4. The dependence of Auger recombination lifetime on Ga composition in n-region at $T = 300$ K, $n = 10^{18}$ cm^{-3}.

of Auger recombination decreases, resulting in the lifetime increasing in the Auger process. Moreover, Fig. 3 shows that Auger recombination lifetime is predominated by the CHHL process in the p-type region, while the CCCH process dominated in the n-type region, is shown in Fig. 4, as explained in the following analysis. Since the CHHL process needs two holes in the valence band and one electron in the conduction band, the CHHL process dominates in the p-type region. On the contrary, the CCCH process needs two electrons in the conduction band and one hole in the valence band; therefore, the CCCH process is playing the main role in the n-type region. In addition, from Eq. (5), it is found that Ga composition has a little influence on τ_{CHHL} because denominator of Eq. (5) is larger in p-type region. Similar conclusion can be drawn for τ_{CCCH} in n-type region. Both are proved by the results shown in Figs. 3 and 4.

Fig. 5(a) provides the dependence of Auger recombination lifetime on Ga composition with carrier concentration of 10^{17}cm^{-3} for both the p- and n-type material at 300 K. It can be seen that the Auger recombination lifetime in the p-type is longer than

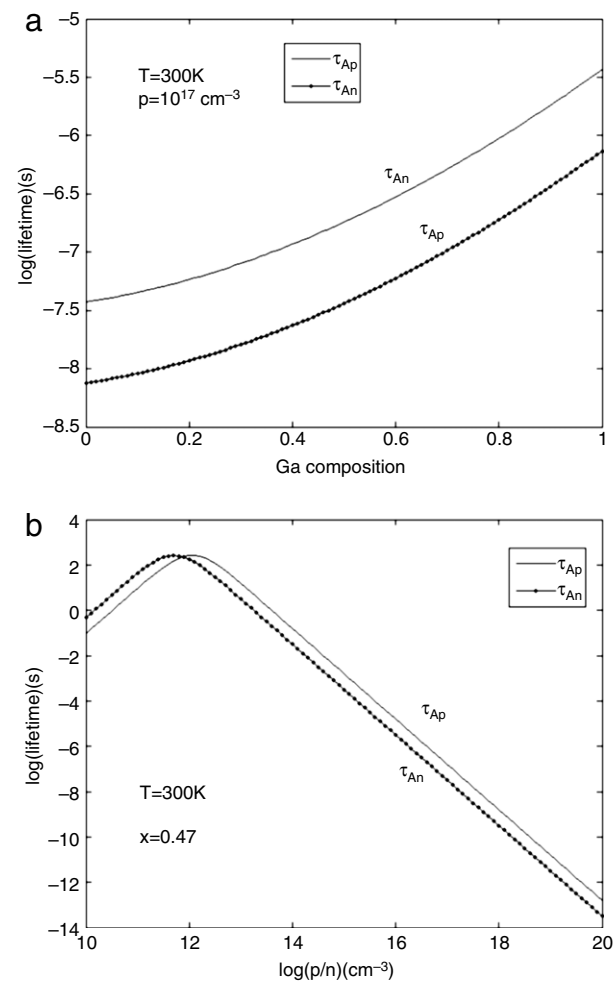

Fig. 5. The dependence of Auger recombination lifetime in the p-type and n-type materials on Ga composition (a) and carrier concentration (b) with $T = 300$ K, $n = p = 10^{17}$ cm^{-3}, $x = 0.47$.

that in the n-type with the same material parameters. Fig. 5(b) shows the dependence of Auger recombination lifetime in the p-type and n-type on the carrier concentrations of $In_{0.53}Ga_{0.47}As$ material at 300 K. The trends for τ_p and τ_n are similar. When the carrier concentration is above 10^{13}cm^{-3}, the Auger recombination lifetimes in the p-type and n-type decrease rapidly with the increasing of carrier concentration. This conclusion has been confirmed in the literature of Metzger et al. [15].

In addition to the Auger recombination lifetime τ_{Auger}, there are other material parameters that also impact R_0A, for instance, the surface recombination velocity and thickness of the material, etc. It is necessary to discuss how these parameters influence R_0A.

In Fig. 6(a) and 7(a), the curves of R_0A versus carrier concentrations of the $In_{0.53}Ga_{0.47}As$ are similar for the p and n regions. When Se, $Sp = 0$,

$$(R_0A)_e \propto \frac{L_e p}{D_e n_i^2} cth\left(\frac{d - w_p}{L_e}\right) \quad \text{(p-region)} \tag{9}$$

$$(R_0A)_h \propto \frac{L_h n}{D_h n_i^2} cth\left(\frac{t - w_n}{L_h}\right) \quad \text{(n-region)} \tag{10}$$

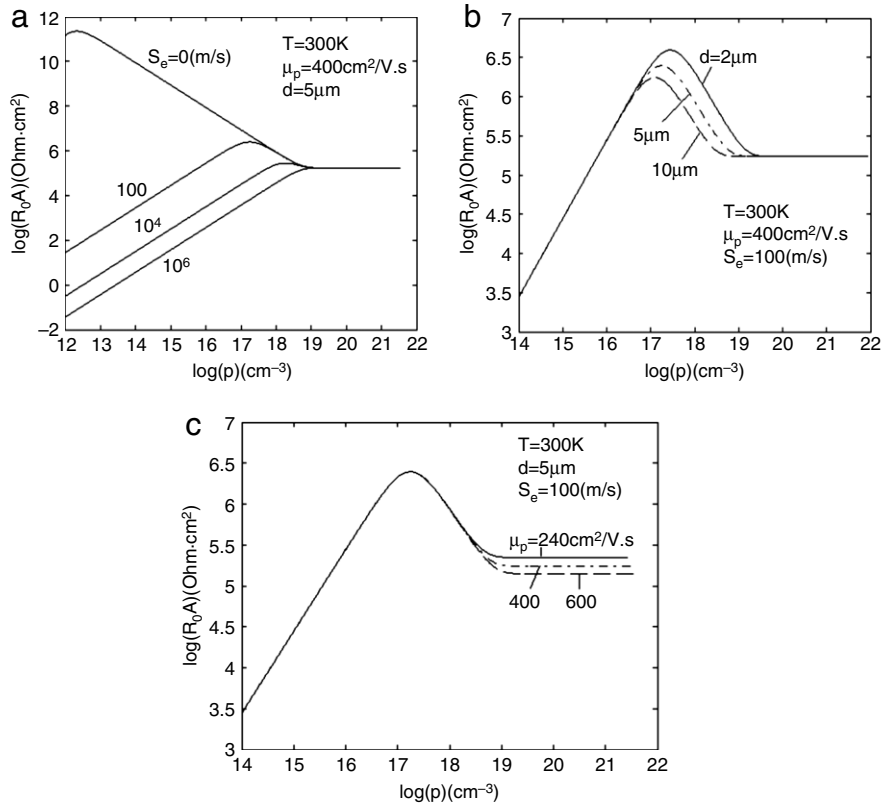

Fig. 6. The dependence of R_0A on material parameters in the p-region with $x = 0.47$.

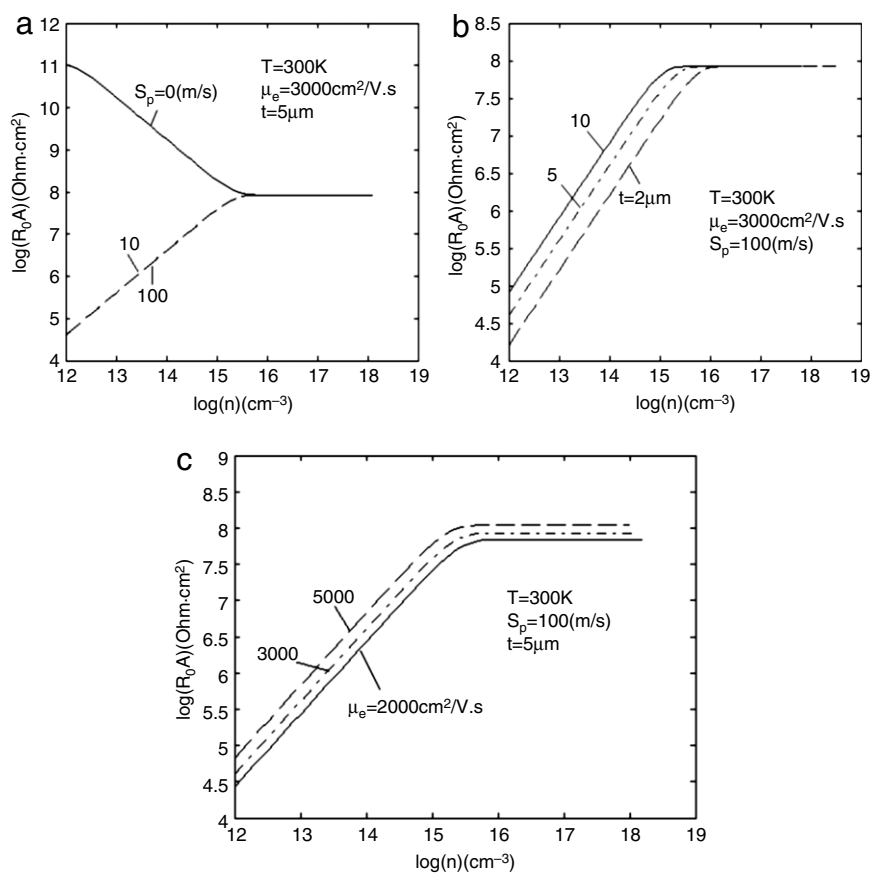

Fig. 7. The dependence of R_0A on material parameters in the n-region with $x = 0.47$.

it makes log(R_0A) decrease with increasing log(p) and log(n) in the carrier concentration range of p or n $< 10^{19}$ cm^{-3}. Moreover, when Se and Sp $\neq 0$,

$$(R_0A)_e \propto \frac{L_e p}{D_e n_i^2} \frac{r_e th\left(\frac{d-w_p}{L_e}\right)+1}{r_e + th\left(\frac{d-w_p}{L_e}\right)} \quad \text{(p-region)} \tag{11}$$

$$(R_0A)_h \propto \frac{L_h n}{D_h n_i^2} \frac{r_h th\left(\frac{t-w_n}{L_h}\right)+1}{r_h + th\left(\frac{t-w_n}{L_h}\right)} \quad \text{(n-region)} \tag{12}$$

log(R_0A) increases with increasing log(p) and log(n) in the carrier concentration range of p or n $< 10^{19}$ cm^{-3}. Reducing surface recombination velocity is benefit to increasing R_0A. Therefore, to improve the performance of the detector, surface passivation processes are essential during device fabrication.

Fig. 6 presents the influence on R_0A by not only the carrier concentration, but also the surface recombination velocity, effective mobility, and thickness of p-region. These influences can be divided into three ranges corresponding to carrier concentration: low carrier concentration range (p $< 10^{16}$ cm^{-3}), high carrier concentration range (p $> 10^{20}$ cm^{-3}) and 10^{16} cm^{-3} $<$ p $<$ 10^{20} cm^{-3} range. In the first range, surface recombination velocity plays the main role in the influence on R_0A. When hole concentration is larger than 10^{20} cm^{-3}, R_0A is affected mainly by mobility. However, in the intermediate range, neither the surface recombination velocity, carrier concentration, nor the thickness of p-type region can be ignored. Similar calculation in n-type region has been presented in Fig. 7. Compared with the impacts on R_0A of material parameters in p- and n-region, two conclusions are obtained: (1) the dependence of R_0A on carrier concentration in n- and p- type regions is similar in the condition of constant surface recombination velocity, (2) R_0A can be achieved with 10^8 Ω cm^2 in n-region, and 10^6 Ω cm^2 in p-region when the surface recombination velocity is 100 m/s. R_0A obtained by the theory is consistent with the experimental values reported by Rogalski et al. [16].

4. Conclusion

The detectivity of photovoltaic detectors at zero-biasing is mainly determined by R_0A, when the background radiation can be negligible. The effect of Auger recombination mechanism on R_0A was analyzed at 300 K in this paper. The results show that the carrier mobility, the absorber thickness, carrier concentration and surface recombination velocity have significant influences to R_0A of an $In_{1-x}Ga_x$ As photodetector lattice-matched to InP substrate. The carrier concentration mainly affects R_0A within the p $< 10^{19}$ cm^{-3} for the p-type in the condition of constant surface recombination velocity. Furthermore, mobility, the absorber thickness and surface recombination velocity have different influences to R_0A in the different carrier concentration regions. The electron mobility has effect on R_0A in larger carrier concentration extent of the n-type. R_0A of 10^6 Ω cm^2 in p-region and 10^8 Ω cm^2 in n-region at $x = 0.47$, can be achieved with the doping level of $10^{17} \sim 10^{18}$ cm^{-3}, when the thickness and the surface recombination velocity of the sample are 5 μm and 100 m/s, respectively. These results provide benefit for design and fabrication of InGaAs detectors.

Acknowledgments

This work was supported by Natural Science Foundation of China Contract No. 60676039, 863 Project of China Contract No. 2009AA03Z442 and 20090422, the Science and Technology Department of Jilin Province under Grant No 20070709.

References

[1] Z.L. Yuan, A.W. Sharpe, J.F. Dynes, A.R. Dixon, A.J. Shields, Appl. Phys. Lett. 96 (2010) 071101.
[2] B. Latika, H. USASMDC, Proc. SPIE 5881 (2005) 588105.
[3] A. Rogalski, Prog. Quantum Electron. 27 (2003) 59–210.
[4] Y.G. Zhang, Y. Gu, Z.B. Tian, K. Wang, A.Z. Li, X.R. Zhu, Y.L. Zheng, J. Crystal Growth 311 (2009) 1881–1884.
[5] J. Kaniewski, J. Piotrowski, Opto-Electron. Rev. 12 (2004) 139–148.
[6] W.K. Metzger, M.W. Wanlass, R.J. Ellingson, R.K. Ahrenkiel, J.J. Carapella, Appl. Phys. Lett. 79 (2001) 3272–3274.
[7] A. Rogalski, R. Ciupaand, W. Larkowski, Solid-State Electron. 39 (1996) 1593–1600.
[8] A. Rogalski, R. Ciupa, J. Appl. Phys. 77 (1995) 3505–3512.
[9] Y. Tian, T.M. Zhou, B.L. Zhang, Y.X. Jin, Y.Q. Ning, H. Jiang, Opt. Eng. 37 (1998) 1754–1762.
[10] A.R. Beattie, J. Phys. Chem. Solids 24 (1962) 1049–1056.
[11] A. Sugimura, J. Appl. Phys. 51 (1980) 4405–4411.
[12] A. Sugimura, IEEE J. Quant. Electron. 18 (1982) 352–363.
[13] T.N. Cassalman, P.E. Peterson, Solid State Commun. 33 (1980) 615–619.
[14] B.L. Gelmont, Phys. Lett. 66A (1978) 323–324.
[15] W.K. Metzger, M.W. Wanlass, R.J. Ellingson, R.K. Ahrenkiel, J.J. Carapella, Appl. Phys. Lett. 79 (2001) 3272–3274.
[16] A. Rogalski, R. Ciupa, J. Electron. Mater. 28 (1999) 630–636.